JCI The Journal of Clinical Investigation

Human acute myelogenous leukemia stem cells are rare and heterogeneous when assayed in NOD/SCID/IL2Rγc-deficient mice

Jean-Emmanuel Sarry, … , G. Danet-Desnoyers, Martin Carroll

Research Article   Hematology

Human leukemic stem cells, like other cancer stem cells, are hypothesized to be rare, capable of incomplete differentiation, and restricted to a phenotype associated with early hematopoietic progenitors or stem cells. However, recent work in other types of tumors has challenged the cancer stem cell model. Using a robust model of xenotransplantation based on NOD/SCID/IL2Rγc-deficient mice, we confirmed that human leukemic stem cells, functionally defined by us as SCID leukemia-initiating cells (SL-ICs), are rare in acute myelogenous leukemia (AML). In contrast to previous results, SL-ICs were found among cells expressing lineage markers (i.e., among Lin$^+$ cells), CD38, or CD45RA, all markers associated with normal committed progenitors. Remarkably, each engrafting fraction consistently recapitulated the original phenotypic diversity of the primary AML specimen and contained self-renewing leukemic stem cells, as demonstrated by secondary transplants. While SL-ICs were enriched in the Lin$^-$CD38$^-$ fraction compared with the other fractions analyzed, SL-ICs in this fraction represented only one-third of all SL-ICs present in the unfractionated specimen. These results indicate that human AML stem cells are rare and enriched but not restricted to the phenotype associated with normal primitive hematopoietic cells. These results suggest a plasticity of the cancer stem cell phenotype that we believe has not been previously described.

Find the latest version:

https://jci.me/41495/pdf

Human acute myelogenous leukemia stem cells are rare and heterogeneous when assayed in NOD/SCID/IL2Rγc-deficient mice

Jean-Emmanuel Sarry,[1] Kathleen Murphy,[1] Robin Perry,[1] Patricia V. Sanchez,[1] Anthony Secreto,[1] Cathy Keefer,[1] Cezary R. Swider,[1] Anne-Claire Strzelecki,[2] Cindy Cavelier,[3] Christian Récher,[2,3,4] Véronique Mansat-De Mas,[2,3,4] Eric Delabesse,[2,3,4] G. Danet-Desnoyers,[1] and Martin Carroll[1]

[1]Division of Hematology and Oncology, Department of Medicine, University of Pennsylvania, Philadelphia, Pennsylvania, USA. [2]Department of Hematology, Centre Hospitalier Universitaire de Toulouse, Hospital Purpan, Toulouse, France. [3]University Paul Sabatier Toulouse III, IFR30, Toulouse, France. [4]INSERM U563, Toulouse, France.

Human leukemic stem cells, like other cancer stem cells, are hypothesized to be rare, capable of incomplete differentiation, and restricted to a phenotype associated with early hematopoietic progenitors or stem cells. However, recent work in other types of tumors has challenged the cancer stem cell model. Using a robust model of xenotransplantation based on NOD/SCID/IL2Rγc-deficient mice, we confirmed that human leukemic stem cells, functionally defined by us as SCID leukemia-initiating cells (SL-ICs), are rare in acute myelogenous leukemia (AML). In contrast to previous results, SL-ICs were found among cells expressing lineage markers (i.e., among Lin+ cells), CD38, or CD45RA, all markers associated with normal committed progenitors. Remarkably, each engrafting fraction consistently recapitulated the original phenotypic diversity of the primary AML specimen and contained self-renewing leukemic stem cells, as demonstrated by secondary transplants. While SL-ICs were enriched in the Lin−CD38− fraction compared with the other fractions analyzed, SL-ICs in this fraction represented only one-third of all SL-ICs present in the unfractionated specimen. These results indicate that human AML stem cells are rare and enriched but not restricted to the phenotype associated with normal primitive hematopoietic cells. These results suggest a plasticity of the cancer stem cell phenotype that we believe has not been previously described.

Introduction

Leukemic stem cells (LSCs) were the first cancer stem cells described, and studies of LSCs have been instrumental in developing the definition of cancer stem cells (1). In 1997, Bonnet and Dick observed that only CD34+CD38− cells were able to reconstitute human acute myelogenous leukemia (AML) in nonobese diabetic mice with severe combined immunodeficiency (NOD/SCID mice) (2, 3). Based on these data, they suggested that LSCs are rare, capable of partial differentiation, and restricted to the immature phenotype associated with hematopoietic stem cells in normal blood differentiation. Subsequent work in other malignancies, also using the NOD/SCID mouse as a model, suggested similar conclusions for breast and colon cancers (4, 5). However, Quintana and colleagues recently reevaluated these results using NOD/SCID/IL2Rγc^null mice (6). In contrast to earlier results, they demonstrate that single melanoma cells, regardless of phenotype, can reconstitute the disease in this more immunocompromised mouse strain. This result has challenged the original concept(s) of cancer stem cell.

Over the last 15 years, immunocompromised mice, such as NOD/SCID mice, have been the model of choice to study morphological and biological characteristics of human AML and other cancers in vivo (3, 7, 8). For AML, however, the engraftment levels in NOD/SCID mice are frequently low, with typical levels ranging from 0.1% to 10% of the mouse BM (7). In addition, prolonged engraftment of leukemic cells in this breed of mice was limited by the development of spontaneous thymic lymphomas and a reduced life span (9, 10). Newer strains of mice engineered with targeted deletion of the β2-microglobulin gene within a NOD/SCID background have resulted in models with decreased NK cell function better suited for studying the progression of diseases such as human AML (11). More recently, reports have demonstrated that a targeted deletion in the γ-common chain in NOD/SCID mice (NSG mice) results in the elimination of residual NK cell activity and provides an improved environment for growth and development of human cells (12, 13). NSG mice are not prone to development of thymomas and have an increased lifespan (12). Engraftment of normal human blood cells is enhanced in these mice, and we and others have demonstrated that AML engraftment is enhanced in this model (14, 15). These observations suggest that the characteristics of the immunodeficient recipient may play an important role in our ability to reveal the functional potential of human LSCs.

The phenotypic characterization of normal and malignant human blood cells has evolved over many years. It was originally observed that selection for CD34+ cells enriched for normal HSCs (16). Subsequent observations showed this population could be further enriched by selecting for lineage-depleted (Lin−) and CD38− cells (17, 18). As noted, the original work on AML stem cells focused on the CD34+CD38− fractions of cells (19). AML cells frequently express markers of granulocytic or monocytic differentia-

Table 1

Clinical, molecular, and engraftment features of 11 primary AML patient specimens used in this work

Collection ID no.	Subtype	Karyotype	Gender	*CD34*	*FLT3*	*NPM1*	*IDH1*	*IDH2*	*CEBPA*	*N-RAS*	*KRAS*	*WT1*	Mouse Engraftment (%)
53	M2	Normal	F	dim	ITD	+	WT	WT	WT	WT	WT	+	43.0
245	M4	Normal	F	dim	ITD	+	R132S	WT	WT	WT	WT	WT	41.1
258	M4	inv(16)(p13;q22)	M	pos	ITD	+	WT	WT	WT	WT	WT	WT	11.8
325	NOS	ND	F	neg	D835	+	R132S	WT	WT	WT	WT	WT	36.0
334	M5	inv(16)(p13;q22)	M	pos	n.d.	n.d.	n.d.	n.d.	n.d.	n.d.	n.d.	n.d.	26.7
348	M2	Normal	F	pos	n.d.	n.d.	n.d.	n.d.	n.d.	n.d.	n.d.	n.d.	31.1
391	M4	t(6;11)(q27;q23), 11q23	M	dim	WT	WT	WT	WT	n.d.	WT	WT	WT	15.3
438	M5	ND	F	dim	ITD	+	WT	WT	WT	WT	WT	WT	10.4
718	M4	Normal	F	dim	ITD	+	R132S	WT	WT	WT	WT	WT	39.3
878	M5	ND	Anonymous	neg	WT	WT	WT	WT	WT	WT	WT	WT	13.2
973	AML-MLD	ND	M	dim	ITD	+	WT	WT	+	WT	WT	+	20.9

n.d., not determined; F, female; M, male; pos, higher than 50% CD34+ cells; dim, 5 to 45% of CD34+ cells; neg, lower than 5% of CD34+ cells.

tion, although expression of these markers is variable within and between samples (20). The role of lineage depletion in enrichment of AML stem cells has not been previously described. Recent studies have suggested the need to reevaluate the phenotypic definition for LSCs. A recent report demonstrates that treatment of AML mononuclear cells with anti-CD38 antibodies prior to transplantation inhibits engraftment in NS mice, suggesting that CD38+ subsets may contain LSCs (21). Also, several groups have shown that treatment of mice with anti-CD44, anti-CD47, or anti-CD123 can inhibit growth of LSCs or their engraftment in NS mice (22–24). It is not clear whether these antibodies interfere with BM homing or stimulation of intracellular signaling or through Fc-mediated clearance of antibody-labeled cells (22). Furthermore, Taussig et al. have observed that both CD34− and CD34+ fractions from the majority of primary *NPM1*-mutated AML contained LSCs (25). Taken together, these results challenge the original phenotypic description of LSCs.

In this study, we demonstrate that human AML stem cells are rare (in contrast to melanoma stem cells) and phenotypically heterogeneous. Our characterization of a diverse set of AML specimens reveals that only a minority of the specimens are strongly positive for CD34 expression, while the majority show low CD34 expression. We have sorted AML cells based on lineage marker, CD34, CD38, and CD45RA expression and tested the capacity of these fractions

to recapitulate the disease in NSG mice. All cell fractions demonstrated some ability to engraft, although results are variable from sample to sample. Quantitative analysis using limiting dilution analysis demonstrated that, although LSCs are found at the highest frequency in the Lin−CD38− fraction, they are not restricted to that fraction. This enriched but rare fraction contains only a minority of the total number of LSCs present in AML cells. The majority of LSCs are found in cell fractions with a more mature phenotype, i.e., expressing CD38 and lineage markers. Remarkably, CD38- and lineage-expressing LSCs can also reconstitute NSG mice with the phenotypic diversity of AML cells found in primary samples, suggesting that LSCs can either dedifferentiate or display lineage infidelity. These data suggest that LSCs are rare, heterogeneous, and may not necessarily arise from primitive hematopoietic cells.

Results

LSCs are rare in human acute myeloid leukemia. We initially performed engraftment analysis on primary specimens from 11 different AML patients, representing multiple different French-American-British (FAB) subtypes (except M3), various karyotypes, and molecular features in terms of the mutational status of 8 genes known to be associated with AML (*FLT3, NPM1, WT1, CEBPA, K-RAS, NRAS, IDH1,* and *IDH2*) (Table 1). All specimens were capable of recapitulating the disease in NSG mice at 12–18 weeks after transplantation, as

Table 2

SL-ICs are rare in human AML

Coll. ID no.	No. of cells injected						Lower limit[A]	Frequency[A]	Upper limit[A]
	50,000	100,000	500,000	1,000,000	5,000,000	10,000,000			
53	1/4	0/5	7/11	6/6	5/5	6/6	762,044	430,240	242,908
245	–	2/5	5/5	5/5	4/4	4/4	366,923	147,704	59,458
325	0/5	2/5	8/8	4/4	5/5	5/5	362,270	180,011	89,447
391	–	–	2/5	4/4	5/5	5/5	1,301,773	559,486	240,460
718	–	0/3	2/4	4/4	3/3	5/5	1,209,858	519,045	337,047
878	1/4	0/4	6/9	3/4	3/5	4/4	3,185,867	1,520,386	725,572
973	–	1/4	0/5	1/5	2/4	5/5	8,611,647	4,122,976	1,973,950

[A]Values represent the number of mononuclear cells for one SL-ICs. Limiting dilution analysis of unfractionated AML samples to determine the frequency of SL-ICs. We injected 50,000–10,000,000 AML cells in adult NSG mice (i.v. tail vein) and analyzed the engraftment level after 12–18 weeks after transplantation. The lower and upper limits of the frequency for each specimen were calculated at 95% CI. Coll., collection.
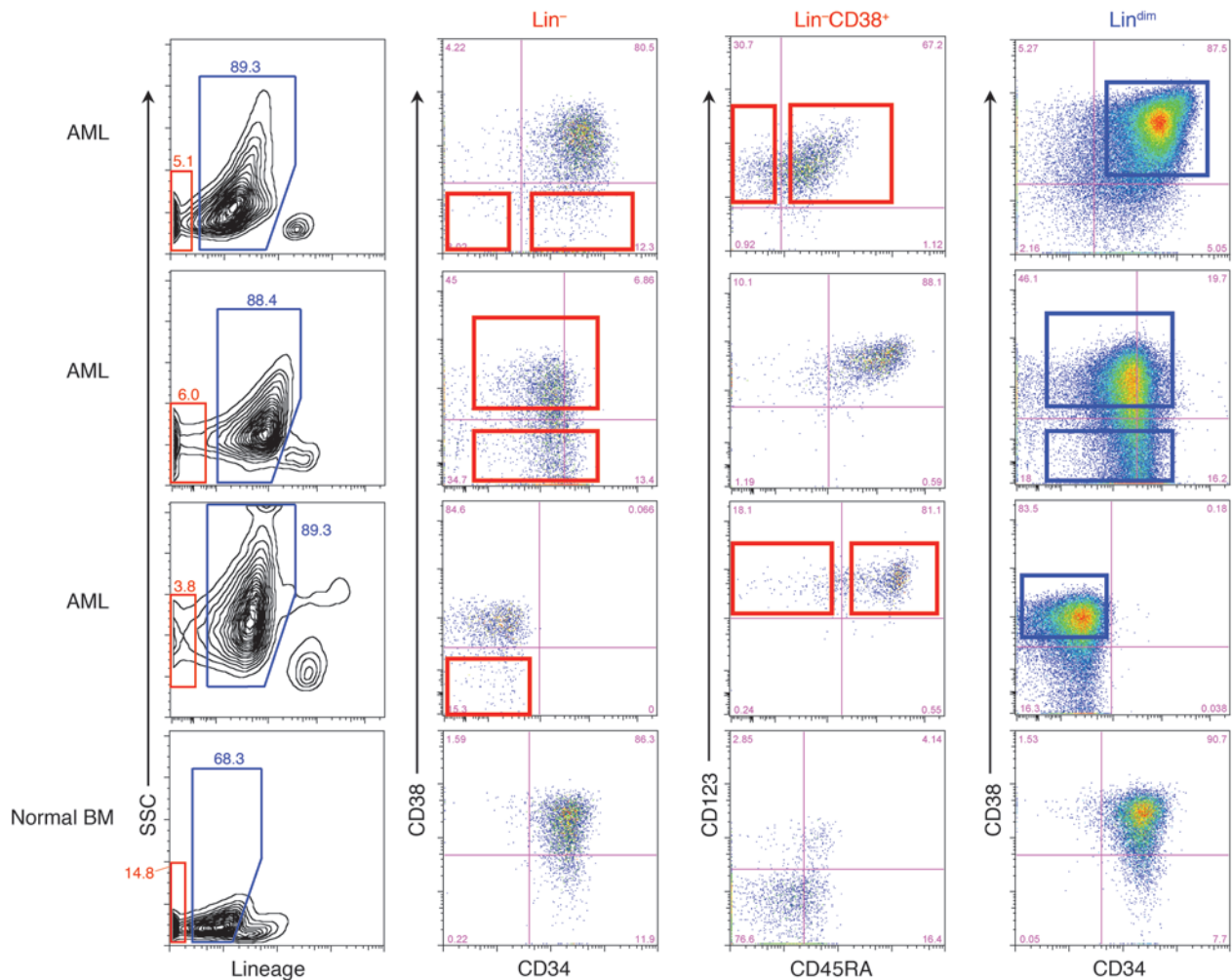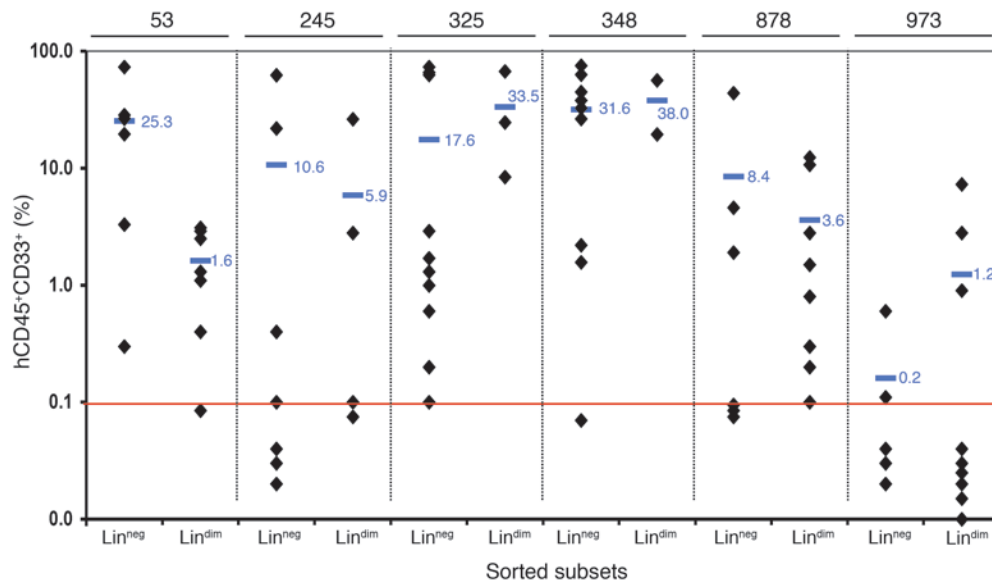
Figure 1
Heterogeneity of the disease immunophenotype compared among patients diagnosed with AML. A representative of CD34[positive] specimen (specimen 348) (top row), a representative of CD34^{dim} specimen (specimen 53) (second row), a representative of CD34[negative] primary specimen (specimen 325) (third row), and an example of CD34^{+}-enriched samples from normal BM (bottom row) are shown. Boxes represent all the different fractions sorted in this study. SSC, side scatter. Numbers in flow plots represent the percent of gated cells within each indicated region.

described previously (14). To determine the frequency of LSCs (functionally defined as SCID leukemia-initiating cells [SL-ICs]) in these specimens, we performed a limiting dilution analysis on unfractionated AML cells from 7 of these samples (Table 2). We injected 50,000 to 10,000,000 AML cells by tail vein injection into adult NSG mice and analyzed the engraftment level after 12–18 weeks after transplantation. The SL-IC frequency in unfractionated samples ranged from 1 SL-IC in 150,000 to 4,500,000 mononuclear cells, confirming that SL-ICs are rare and that the frequency varies broadly between patients (Table 2).

AML cells are phenotypically heterogeneous. To evaluate the diversity of AML cell phenotypes, we analyzed primary AML specimens for expression of cell surface markers used to enrich for normal BM stem cells and progenitors. We included lineage markers (as a cocktail of CD3, CD14, CD16, CD19, CD20, and CD56 to identify mature lymphocytes and myeloid cells), CD34, CD38, CD123, and CD45RA. These markers are used in normal BM to distinguish stem cells and primitive progenitors (Lin⁻CD34⁺CD38⁻) from more mature progenitors (CD34⁺CD38⁺), including common myeloid

progenitors (CMPs) (CD34⁺CD38⁺CD45RA⁺CD123⁻) and granulocyte-monocyte progenitors (GMPs) (CD34⁺CD38⁺CD45RA⁺ CD123⁺) (26). An example of such phenotyping using CD34⁺-enriched samples from normal BM is shown in Figure 1 (bottom row). We then studied the phenotype of 19 primary AML specimens, and we consistently found 3 distinct populations based on the expression of lineage markers: a lineage bright (Lin⁺) population composed of mature lymphocytes (mostly CD3⁺ and CD19⁺ cells), a population with low expression of lineage markers (Lin^{dim}), and a lineage-negative (Lin⁻) population (Figure 1, first column). We further focused on the lineage dim and lineage-negative fractions to determine the pattern of CD34 expression. We observed that CD34 expression is highly variable between specimens (Figure 1, second column). These AMLs were subdivided into 3 groups based on CD34 expression: (a) samples with a high level of CD34 expression, such as specimen 348, were the least frequent (21%, 4 out of 19 specimens); (b) those with dim CD34 expression, such as specimen 53, were the most common (47%, 9 out of 19); and (c) AMLs with no CD34 expression, representing 32% (6 out of 19) of the specimens evalu-
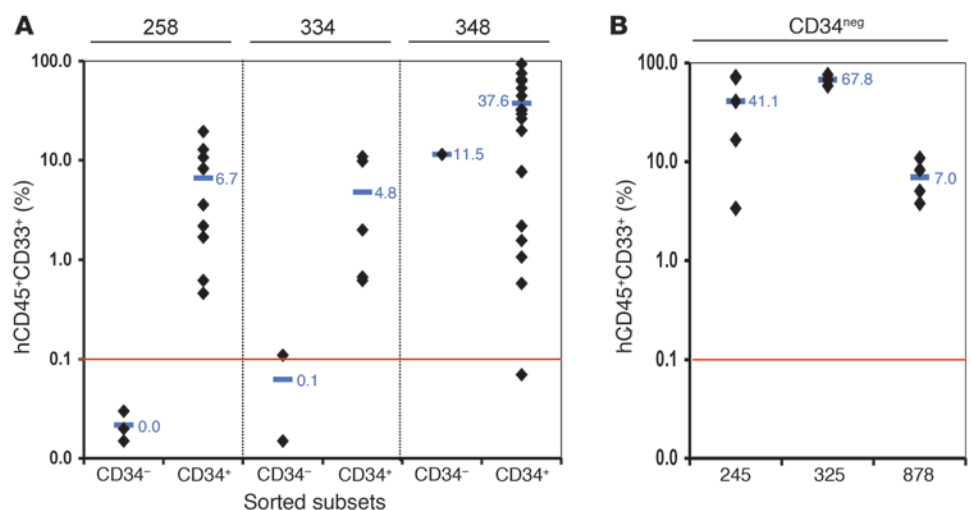
Figure 2
Engraftment level of human AML cells in BM of NSG mice after 12 weeks after transplantation of Lin^negative and Lin^dim subsets sorted from 6 primary AML patient samples. Black diamonds show the engraftment level in each individual mouse, injected with at least 0.3 million sorted human cells. Numbers above each graph indicate the specimen identification number. Numbers by each horizontal bar indicate the mean of human blast engraftment in NSG mice for each sorted and injected fractions.

ated. For each sample, the CD34 expression pattern was the same in the Lin⁻ and Lin^dim fractions (Figure 1, compare second and fourth columns). These results demonstrate that CD34 expression is highly variable among AML samples. Furthermore, since all the samples were capable of engrafting in NSG mice, our results indicate that, in 32% of the samples, SL-ICs did not express CD34. In contrast to CD34 expression, all the AML samples had a similar pattern of CD38 expression, with a majority of CD38⁺ cells in both Lin⁻ and Lin^dim fractions (Figure 1). Finally, we also characterized the expression of CD45RA and CD123 in the Lin⁻CD38⁺ fractions to evaluate the presence of cells with myeloid progenitor-like phenotypes (Figure 1, third column). Regardless of their CD34 expression status, we observed a CD123⁺CD45RA⁺ population in all samples. Overall, these results illustrate the heterogeneity of phenotypes in AML

samples. The absence of CD34 expression in some samples capable of engrafting in NSG mice led us to reevaluate and ask whether SL-ICs are completely restricted to the immature cell phenotype.

SL-ICs are found in both Lin⁻ and Lin^dim fractions. To determine whether SL-ICs were restricted to a population of cells that do not express lineage markers (Lin⁻), we first sorted Lin⁻ and Lin^dim cells from 6 different primary AML samples and injected 0.1×10^6 to 4.3×10^6 cells per mouse (Figure 2). To ensure that these and other sorted cells did not have contamination, postsorting cell purity was checked for all samples and averaged at least 95% pure (Supplemental Table 1; supplemental material available online with this article; doi:10.1172/JCI41495DS1). Surprisingly, for each sample, both Lin⁻ and Lin^dim fractions were capable of recapitulating the disease, demonstrating that SL-ICs are not only found in

Figure 3
SL-IC do not necessarily express CD34. Engraftment level of human AML cells in BM of NSG mice 12 weeks after transplantation of CD34⁻ and CD34⁺ subsets sorted from 6 primary AML patient samples expressing (**A**) CD34 or (**B**) not. Black diamonds show the engraftment level in each individual mouse, injected with 0.1 to 1.0 million sorted human cells.
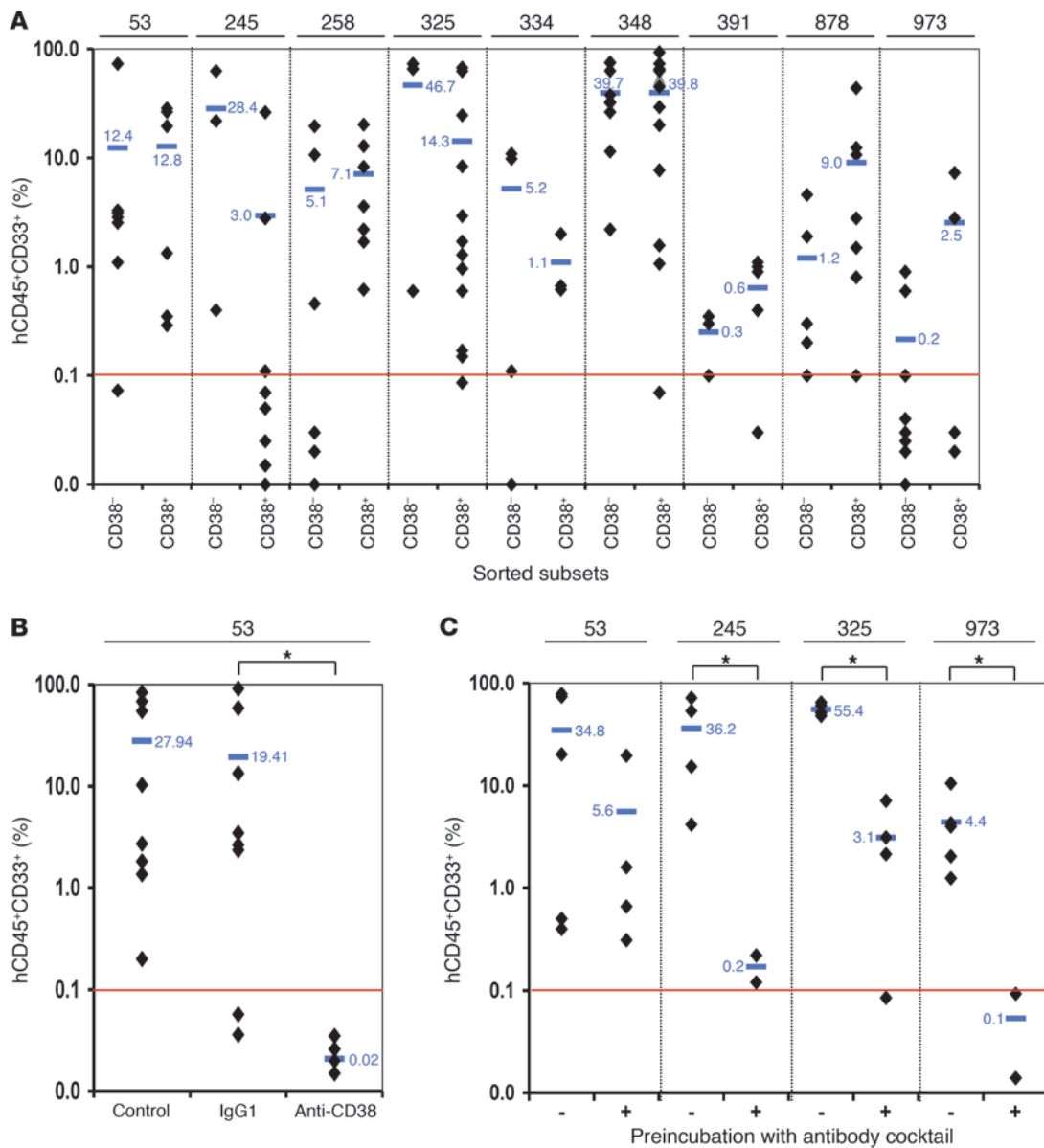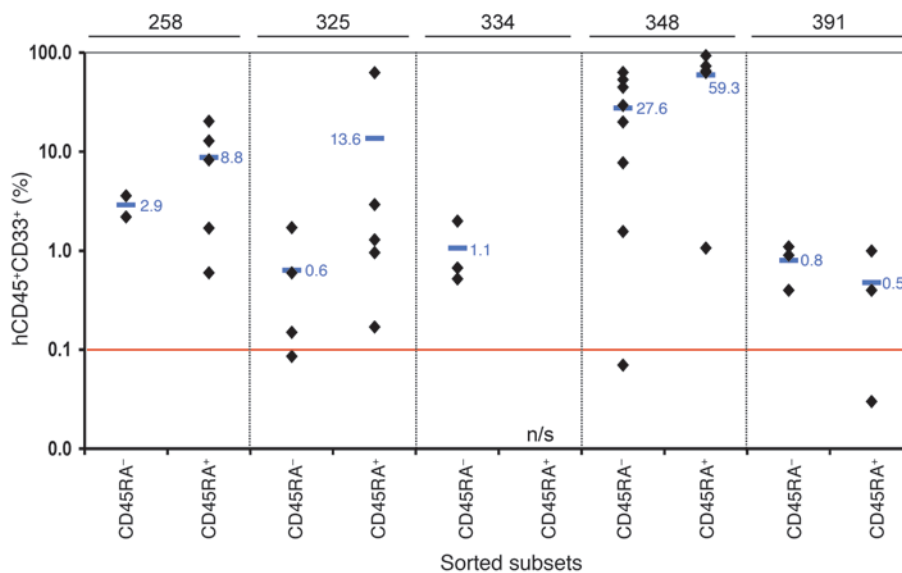
Figure 4
SL-ICs are not restricted to CD38⁻ populations. (**A**) Engraftment level of human AML cells in BM of NSG mice after 12 weeks after transplantation of CD38⁻ and CD38⁺ subsets sorted from AML primary samples. (**B**) Sixteen-hour incubation of AML mononuclear cells from primary specimen 53, with anti-CD38 antibody affects the human cell engraftment in NSG mice. (**C**) Comparison of the engraftment level after 12 weeks after transplantation of unsorted, unstained (–) samples versus unsorted, stained (+) samples for 4 primary AML specimens. Black diamonds show the engraftment level in individual mice, injected with 0.1 to 1.0 million sorted human cells. *$P < 0.05$, Mann-Whitney U test.

the rare Lin⁻ fraction but also in the more abundant Lindim population. Interestingly, Lindim cells from samples 325 and 348 provided a higher level of leukemia engraftment than Lin⁻ cells when injected at similar doses in NSG mice. This suggests that in these samples SL-ICs could be as frequent in the Lindim fraction as in the Lin⁻ fraction. Overall, these data demonstrate that both Lin⁻ and Lindim fractions contain SL-ICs, suggesting that expression of lineage markers associated with commitment and differentiation is not necessarily associated with a loss of LSC function.

SL-ICs are not restricted to CD34⁺ cells. Next, we examined whether SL-ICs were restricted to CD34⁺ cells in AML samples with high

CD34 expression. In normal human hematopoiesis, SCID-repopulating cells (SRCs) are most abundant in the Lin⁻CD34⁺CD38⁻ fraction, although rare SRCs have been reported in Lin⁻CD34⁻ cells (18). As noted, only a minority of samples demonstrated robust CD34 positivity. These samples had few CD34⁻ cells, making analysis of CD34⁻ engraftment challenging. Nonetheless, 3 primary AML CD34⁺ specimens were sorted based on their CD34 expression. To isolate CD34 as a variable, we compared CD34⁻38⁻ cells with CD34⁺CD38⁻ cells as shown in Figure 1. Only 2 mice of 6 injected with CD34⁻ cells showed a significant engraftment (higher than 0.1% of human cells in murine BM), consistent with the idea

Figure 5
Engraftment level of human AML cells in BM of NSG mice 12 weeks after transplantation of CD38+CD45RA− and CD38+CD45RA+ subsets sorted from 5 AML primary samples. Black diamonds show the engraftment level in each individual mouse, injected with 0.1 to 1.0 million sorted human cells.

that, in the subset of AML samples with clear CD34+ staining, SL-ICs are depleted in the CD34− fraction (Figure 3A). As expected, 36 out of 37 mice injected with their CD34+ counterpart engrafted in mice (Figure 3A). To next determine whether CD34 staining is necessary for the LSC phenotype, we characterized the engraftment of CD34^{negative} samples. In these samples, insufficient CD34+ cells are present to allow for separate analysis of engraftment of rare CD34+ cells from these patients. All mice injected with CD34^{negative} specimens engrafted in NSG mice after 12 weeks after transplantation (Figure 3B). Taken together, these data suggest that, in a subset of AML samples with a clear CD34^{positive} fraction of cells, CD34 staining enriches for SL-ICs. However, expression of CD34 is not necessary for engraftment potential. Rather, these data demonstrate the phenotypic heterogeneity of AML samples.

Expression of CD38 and CD45RA on SL-ICs. Although the phenotype of SL-ICs was originally described as CD38−, recent data showing that preincubation of AML cells with an anti-CD38 antibody can suppress engraftment led us to reevaluate whether SL-ICs are indeed restricted to CD38− cells (21). AML samples from 9 patients were sorted into CD38− and CD38+ fractions, and cells from each fraction were injected into NSG mice. As demonstrated in Figure 4A, SL-ICs were not restricted to CD38− cells, as the CD38+ fraction tested was capable of recapitulating the disease in NSG mice. Remarkably, CD38+ cells provided levels of engraftment equal or superior to the levels observed with CD38− cells in 5 out of the 9 patients. These results may under-represent the engraftment potential of CD38+ cells to engraft, since Taussig et al. demonstrated that incubation of human AML cells with anti-CD38 antibodies, but not control antibodies, decreased engraftment (21). We confirmed this observation by incubating AML samples overnight with the anti-CD38 antibody (HIT2 clone). As shown by Taussig and colleagues, this incubation abrogates engraftment of both AML samples tested (Figure 4B and ref. 21). Overall, these results demonstrate that SL-ICs are present in the CD38+ fraction of AML cells.

These results made us question whether there is a specific cytotoxic effect of the HIT2 anti-CD38 antibody or whether antibody labeling of AML cells generally decreases engraftment. We analyzed the impact of incubation of AML cells with an antibody cocktail (lineage, CD34, CD38, CD123, and CD45RA) used for sorting on

engraftment levels in NSG mice (Figure 4C). In 4 patient samples, we observed that a 1-hour incubation with these antibodies significantly decreased the level of engraftment 12 weeks after transplantation. We next performed a limiting dilution analysis of 2 specimens (specimens 53 and 325) after incubation with these antibodies and observed that the frequency of SL-ICs was not affected (Supplemental Table 2). Taken together, these results suggest that incubation of AML cells with antibodies can qualitatively affect the level of engraftment (as evaluated 12 weeks after injection) but does not quantitatively affect SL-IC levels.

These results show that the use of antibodies impairs our ability to reveal the full potential of CD38-expressing SL-ICs, suggesting caution in interpreting quantitative studies aimed at determining the frequency of SL-ICs in such fraction. To explore this further, we studied whether CD38 expression is reversible and dependent on cell cycle status, as previously demonstrated in normal CD34+ cells by McKenzie et al. (27). While the expression of CD38 is highest in cells in G_2/M in most samples, we did not observe a consistent difference in expression of CD38 between cells in G_0 and G_1 from 6 samples (Supplemental Figure 1). Overall, there does not appear to be a robust correlation of CD38 expression with cell cycling in AML cells.

Studies in murine models of leukemia have demonstrated that SL-ICs can be found in cell fractions with phenotypes associated with CMPs or GMPs. In humans, CMPs and GMPs express CD34, CD38, and CD123 and vary in expression of CD45RA. In AML samples with a clear CD34+CD38+ population, we further sorted cells based on CD45RA expression and analyzed their engraftment potential in NSG mice. As shown in Figure 5, in 4 patients, SL-ICs could be detected in both CD45RA+ and CD45RA− fractions, indicating that, within the CD34+CD38+ fraction, SL-ICs are found in both CMP-like and GMP-like cells. Furthermore, SL-ICs were also found in both CD45RA+ and CD45RA− fractions from 1 AML specimen, which is CD34^{negative} sample 325. Thus, similar to murine models of leukemia, SL-ICs can be found in phenotypic CMPs and GMPs in human AML.

SL-ICs reconstitute the disease heterogeneity. To determine whether each engrafting fraction could reconstitute the phenotypic heterogeneity of the original AML sample, we compared the phenotypes of the AML cells before and 12 weeks after transplan-
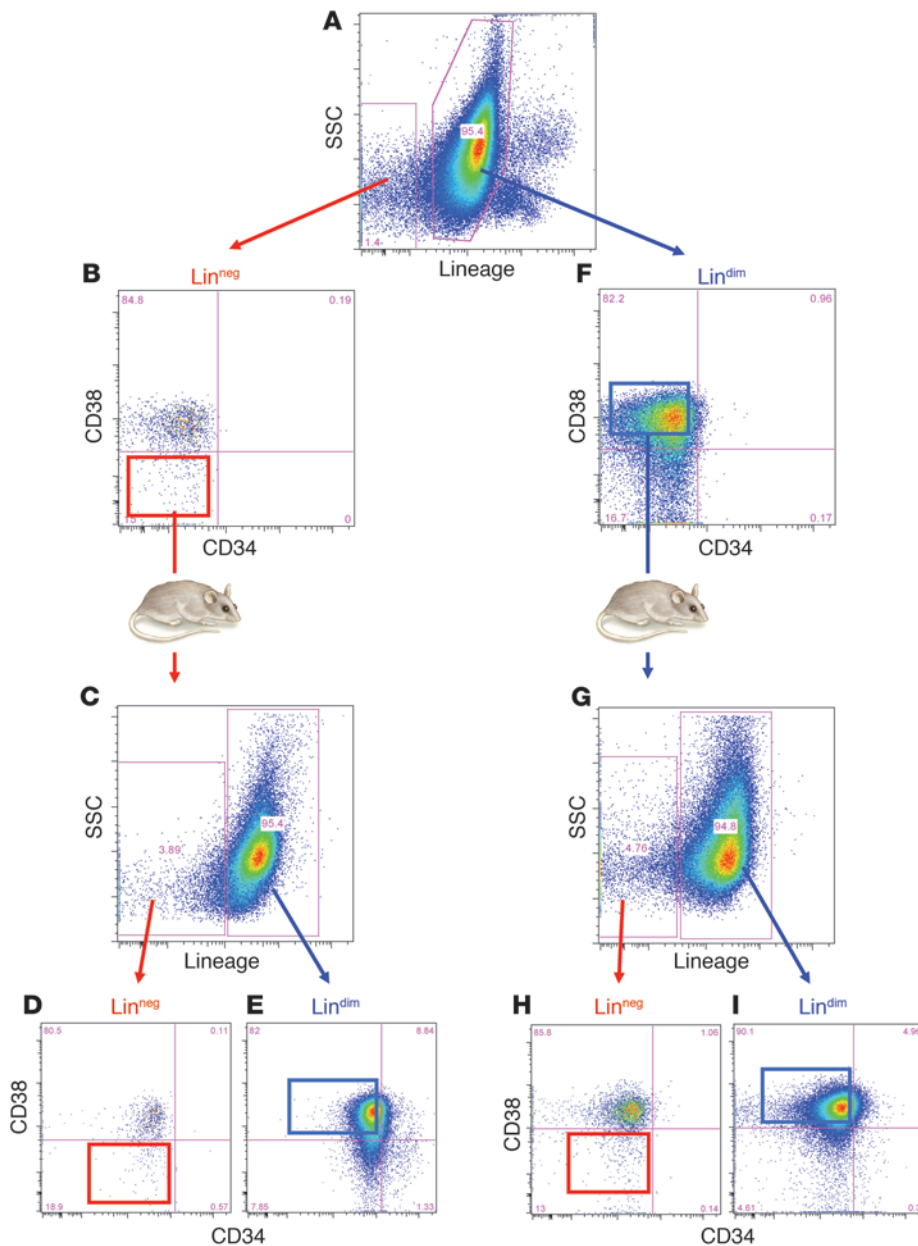
Figure 6
Reconstitution of the original AML phenotype from all sorted fractions from CD34^negative specimen 325. (**A**, **B**, and **F**) Original immunophenotype of the patient cells. (**C**–**E**) Phenotype of BM cells from NSG mice injected with Lin⁻CD38⁻ cells and harvested 12 weeks after transplantation. (**G**–**I**) Phenotype of BM cells from NSG mice injected with Lin^dimCD38⁺ cells and harvested 12 weeks after transplantation. Numbers in flow plots represent the percent of gated population within each indicated region.

tation. We observed that each sorted fraction was capable of reconstituting the mice with AML cells with the same phenotypic diversity seen in the unsorted primary AML samples (see a representative example with sample 325 in Figure 6). For example, Lin⁻CD38⁻ cells (Figure 6, A and B) injected into mice gave rise to Lin⁻CD38⁻ (Figure 6, C and D), Lin⁻CD38⁺ (Figure 6, C and D), and Lin⁺ cells (Figure 6, C–E) at 12 weeks after transplantation. Interestingly, Lin^dimCD38⁺ cells (Figure 6, A–F) gave rise to both Lin^dimCD38⁺ cells (Figure 6, G–I) and Lin⁻CD38⁻ cells (Figure 6, G and H) after 12–16 weeks. Moreover, these 2 populations arising from Lin^dimCD38⁺ cells represent approximately the same percentages of total AML cells in the primary sample and at 12 weeks after transplant. These results demonstrate that each cell fraction tested for engraftment in NSG mice could closely recapitulate the phenotypic diversity of AML cells observed in primary samples, fulfilling one of the criteria of a LSC.

Next, we used transplantation into secondary NSG recipients to assess the self-renewal capacity of SL-ICs in different sorted fractions from 5 samples. All engrafting subsets from primary recipients were capable of engraftment in secondary recipients (Table 3), showing that the sorted fractions contained SL-ICs capable of both recapitulating the phenotypic heterogeneity of the primary AML and self-renewal. For 3 cases (sample 53 [with the mutations *FLT3*-ITD, *NPM1c*, *WT1* exon 7], sample 325 [with the mutations *FLT3*-TKD, *NPM1c*, *IDH1* R132S], and sample 973 [with the mutations *FLT3*-ITD, *NPM1c*, *WT1* exon 7]), we were able to check the presence of mutations in sorted cell fractions from primary and secondary NSG recipients (Supplemental Table 3). For samples 53 and 973, the 3 mutations were present in every sorted fraction tested. For sample 325, only the IDH1 R132S and NPM1c mutations were still present in all sorted fractions of patient sample and engrafted mice recipients. In contrast, the FLT3-TKD muta-

Table 3
All engrafting subsets contain self-renewing LSCs

| Coll no. | FAB | Lin negative fractions | | | | | | | | Lin dim fractions | | | | |
| | | CD38− | | | CD38+ | | | | | CD38− | | | CD38+ | |
		CD34−	CD34dim	CD34+	CD34dim	CD34− CD45RA−	CD45RA+	CD34+ CD45RA−	CD45RA+	CD34dim	CD34− CD45RA−	CD45RA+	CD34−	CD34dim
258	M4			+ (2/2)				+ (1/1)	+ (2/2)					
334	M5			+ (2/2)				+ (1/1)						
348	M2	+ (1/1)		+ (4/5)				+ (3/4)	+ (2/2)					
53	M2	+ (3/3)	+ (4/4)		+ (3/3)								+ (3/3)	
325	NOS	+ (3/3)						+ (3/3)	+ (3/3)			+ (3/3)	+ (3/3)	+ (5/5)

We injected 1,000,000 to 10,000,000 human CD45+CD33+ viable cells from BM of primary recipients per mouse (i.v. tail vein) and analyzed the engraftment level after 12–18 weeks after transplantation. A + sign indicates that self renewing cells were present in the indicated fractions of cells. The numbers in parenthesis represent the number of engrafted mice per injected mice. ITD, internal tandem duplication; TKD, tyrosine kinase domain; IDH1, isocitrate dehydrogenase 1; R132S, arginine 132 serine mutation.

tion in this case was uniquely present in sorted fractions coming from the primary recipient but was absent in all fractions of the secondary recipient, suggesting that in this 1 sample, expression of mutant Flt3 is not necessary for a stem cell phenotype. The ability to reconstitute animals long term after secondary transplantation, along with the ability to develop a diverse phenotype that recapitulates the original disease phenotype, ensures that the cell fractions studied in these experiments represent bona fide SL-ICs and not transient populations.

Quantitative analysis of SL-ICs in discrete cell fractions. To determine whether SL-ICs are preferentially enriched in specific fractions, we used cells from sample 53 to perform a limiting dilution analysis on 4 fractions based on lineage and CD38 expression followed by injection in NSG mice (Table 4). The frequency of SL-ICs in each fraction was calculated using regression analysis (L-Calc). We observed that Lin−CD38− cells contained the highest frequency of SL-ICs (1 in 38,030 cells) compared with that of Lin^{dim}CD38− cells (1 in 372,259 cells) and Lin−CD38+ cells (1 in 345,807 cells). The fraction with the lowest frequency of SL-ICs was Lin^{dim}CD38+ (1 in 1,023,815 cells). In comparison, the frequency of SL-ICs in unfractionated cells was 1 in 430,240 (Table 2). This demonstrates that SL-ICs are indeed enriched in the Lin−CD38− fraction in this sample. Considering that the incubation of AML cells with an anti-CD38 antibody can decrease engraftment in NSG mice, the frequency of SL-ICs in both CD38+ subsets may be underestimated. We used the SL-IC frequency and the percentage of the total cells found in each phenotype to calculate the absolute numbers of SL-ICs associated with each fraction for specimen 53. For instance, Lin−CD38− cells contain the highest frequency of SL-ICs (1 in 38,030 cells), with 11-fold enrichment compared with that of the unfractionated sample (Supplemental Table 5). However, Lin−CD38− cells represent only 3% of all mononuclear cells in patient 53 (Figure 7, top bar). Normalizing to 100 SL-ICs, we determined that, in spite of having the highest frequency of SL-ICs, the Lin−CD38− fraction contains only 34% of all SL-ICs (Figure 7, bottom bar). In comparison, the Lin^{dim}CD38+ fraction contains the lowest frequency of SL-ICs, but it is the most represented fraction in patient 53 (61% of cells; Figure 7, top bar) and contains 25% of all SL-ICs (Figure 7, bottom bar). Overall, the CD38+ and Lin^{dim} fractions contain 29% and 62% of all SL-ICs, respectively. Assuming that we sort each fraction from 100×10^6 cells (containing 332 SL-ICs at the frequency of 1:430,240), Lin−CD38− fraction will contain 61×10^6 total AML cells and 79 SL-ICs at the frequency of 1:38,030 (Supplemental Table 4). Thus, the total number of SL-ICs summed from all sorted fractions is 236 SL-ICs (e.g., 71% of the total number of SL-ICs presorting; Supplemental Table 4). These data demonstrate that SL-ICs are widely distributed throughout different phenotypes and that the absolute distribution of LSCs does not correlate with immunophenotypic distribution (Figure 7). Importantly, at least one-third of SL-ICs detected in the NSG model are found in CD38+ fractions previously described as devoid of LSC activity.

Of note, we had several cell doses for Lin−CD38− and Lin−CD38+ subsets from 4 additional specimens, although we were not able to do a complete LDA on these samples (Supplemental Table 5). This data allowed us to approximate the SL-IC frequency in several fractions of these samples. We observed the highest frequency of SL-ICs in Lin−CD38− in 1 sample (sample 973), similar frequency in both fractions in 1 sample (sample 348), and the lowest frequency in Lin−CD38− from a 3rd sample (sample 258). Although not conclusive, this data suggests that the degree of enrichment

Table 4

SL-ICs are enriched in a Lin⁻CD38⁻ subset

Fractions	No. of cells injected					Lower limit[A]	Frequency[A]	Upper limit[A]
	10,000	50,000	100,000	500,000	1,000,000			
Lin^{dim}CD34^{dim}CD38^{+}	–	–	0/4	2/4	5/5	2,512,183	1,023,815	417,246
Lin^{dim}CD34^{dim}CD38^{-}	–	0/4	1/4	5/7	4/4	744,071	372,259	186,241
Lin^{negative}CD34^{dim}CD38^{+}	–	0/2	1/4	2/3	5/5	788,499	345,807	151,659
Lin^{negative}CD34^{dim}CD38^{-}	1/4	4/4	3/4	8/8	–	86,997	38,030	16,625

[A]Values represent the number of MNCs for one SL-ICs. Limiting dilution analysis of sorted fractions from 1 primary AML sample (sample 53). We injected 10,000 to 1,000,000 AML cells from 4 different sorted fractions in adult NSG mice (i.v. tail vein) and analyzed the engraftment level after 12–17 weeks after transplantation. Lower and upper limits of the frequency for each fraction were calculated at 95% CI. The numbers in parenthesis represent the number of engrafted mice per injected mice.

of SL-ICs in the immature, Lin⁻CD38⁻ fraction, as assayed in the NSG mouse, may be highly variable. Overall, our results indicate that in AML, LSCs are rare, heterogeneous in phenotype, and may be distributed through multiple compartments of AML cells.

Discussion

In this study, we have reexamined the characteristics of LSCs in human AML using the NSG xenotransplantation model. Recent results from our laboratory have demonstrated enhanced engraftment of primary AML specimens in NSG mice compared with that in NOD/SCID mice, suggesting that the functional assay used to measure LSCs may be more sensitive in the NSG model than in the NOD/SCID model (14). In spite of this enhanced sensitivity, our quantitative analysis of SL-IC frequency in a diverse group of 7 AML patients shows that LSCs are rare cells within AML samples (range, 1 in 0.15×10^6 to 4.1×10^6 LSCs). The rarity of SL-ICs in AML has been a consistent finding regardless of the strain of immune-deficient mice used over the past 15 years. Lapidot et al. used SCID mice to estimate the frequency of SL-ICs at 1 in 2.5×10^5 (19). When NOD/SCID mice were used, SL-IC frequencies ranged from 1 SL-IC in 10^4 cells to 1 in 1.4×10^7 cells (3, 7). Overall, these results indicate that the use of increasingly immunodeficient and permissive mouse strains to assay AML-initiating cells is not associated with an increase in the frequency of SL-ICs. This is in contrast with a recent report on human melanoma, showing that the use of NSG mice instead of NOD/SCID mice increased the frequency of tumorigenic cells by several orders of magnitude (6). These contrasting results between AML and melanoma in NSG mice could reflect the fact that the microenvironment in this strain is particularly favorable to melanoma cell growth. Human AML stem cells remain a rare population of cells.

We demonstrate that the phenotype of LSCs is heterogeneous and not restricted to the immature phenotype CD34⁺CD38⁻ as originally described by Bonnet and Dick (3). We report here that for each sample evaluated SL-ICs are consistently found in both Lin⁻ and Lin^{dim} fractions, indicating that the transition to lineage marker expression is not necessarily associated with a loss of capacity to initiate AML. Remarkably, we found that none of the cell surface markers (Lin, CD34, CD38, CD45RA, and CD123) used to identify hematopoietic stem cells and myeloid progenitors in normal BM could be used to consistently segregate AML-initiating and self-renewing cells. The heterogeneity in CD34 and CD38 expression within and between AML specimens has been previously reported (28). Interestingly, the 3 specimens (specimens 245, 325, and 878) devoid of CD34⁺ cells engrafted well in NSG mice,

indicating that AML-initiating cells do not necessarily express CD34. We found that, in specimens containing both CD34⁺ and CD34⁻ cells, SL-ICs could be found in both fractions, as reported by Terstappen et al. (17) and Blair et al. (28). At this time, we can not directly address whether the difference between our results and the original model proposed by Bonnet and Dick is a consequence of the switch to the NSG mouse model for xenotransplantation or the heterogeneity of the disease, since we have not tested the AML fractions studies here for engraftment in NOD/SCID animals.

Taussig et al. recently reported that CD34⁺CD38⁺ cells can recapitulate AML in NSG mice, but they did not evaluate the self-renewal capacity of these cells (21). We demonstrate that both CD38⁻ and CD38⁺ fractions contain SL-ICs for all 9 samples evaluated. In addition, we report that CD38⁺ cells are capable of self-renewal as revealed by long-term AML engraftment in secondary recipients and, importantly, that CD38⁺ cells will reconstitute
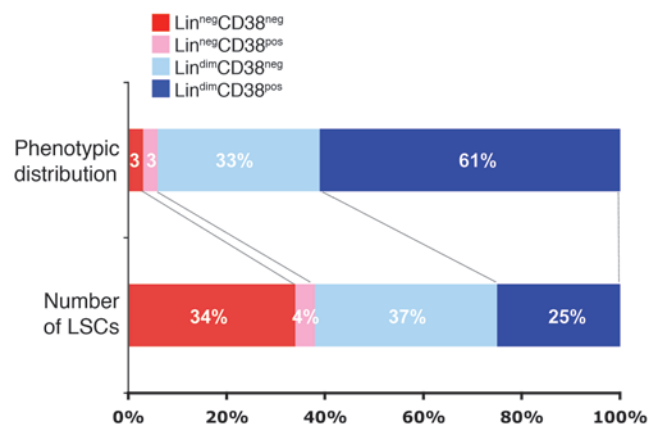

Figure 7

The absolute distribution of SL-ICs does not correlate with their immunophenotypic distribution. We assessed the percentage of the total cells found in each phenotype by extensive flow cytometry (top bar). Subsequently, we calculated the absolute numbers of SL-ICs associated with each fraction (bottom bar) using the SL-ICs frequency and the percentage of the total cells found in each phenotype. For instance, Lin⁻CD38⁻ cells contain the highest frequency of SL-ICs (1 in 38,030 cells); however, Lin⁻CD38⁻ cells represent only 3% of all mononuclear cells in patient 53 (top bar). Normalizing to 100 SL-ICs (i.e., 100 × [1/430,240] = 43×10^6 mononuclear cells), we determined that, in spite of having the highest frequency of SL-ICs, the Lin⁻CD38⁻ fraction contains only 34% ($43 \times 10^6 \times 0.03/38,030 = 34$) of all SL-ICs (bottom bar).
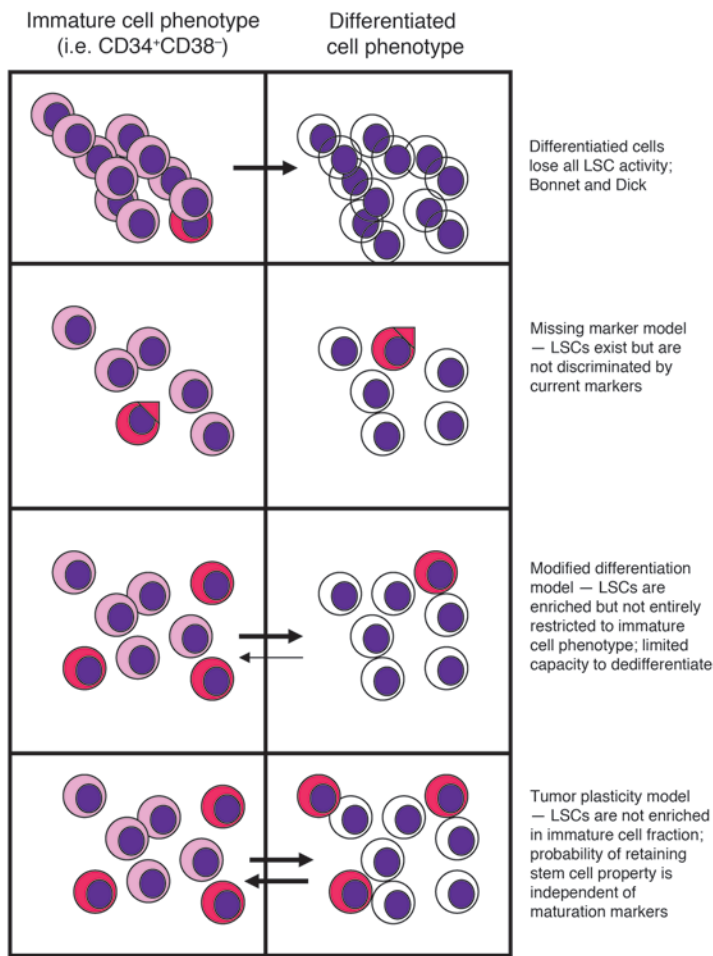
Figure 8
Proposed models for leukemic stem hypothesis. The original model described a binary model of tumor heterogeneity, with most differentiated cells losing all LSC activity (top row). LSCs exist but are not discriminated by current markers (missing marker model; second row). LSCs are enriched but not entirely restricted to immature cell phenotype, with limited capacity to dedifferentiate (modified differentiation model; third row). LSCs are not enriched in the immature cell fraction; probability of retaining stem cell property is independent of maturation markers (tumor plasticity model; bottom).

of SL-ICs with myeloid progenitor-like phenotypes strengthen the concept that AML-initiating cells are not necessarily derived from hematopoietic stem cells as initially hypothesized (3). It remains unclear whether SL-ICs can originate directly from the transformation of committed myeloid progenitors, as shown in mouse models. Alternatively, SL-ICs could originate first from normal hematopoietic stem cells and then, as a secondary event, from preleukemic progenitors acquiring self-renewal capacity (29).

The data described here present a fundamental challenge to the LSC model as it was originally proposed. The original model described a binary model of tumor heterogeneity in which there were cells capable of tumor reconstitution in a NOD/SCID mouse (stem cells) and cells that had no capacity for tumor reconstitution (Figure 8, top). Furthermore, LSCs were proposed to reside only in the immature compartment of hematopoietic cells, suggesting that limited differentiation within tumor cells recapitulated normal hematopoietic differentiation. In contrast, our results demonstrate that cells with features resembling a more mature hematopoietic cell can reconstitute a leukemia within the more sensitive NSG mouse model. There are 3 possible explanations. It is possible that the original model is correct in that there are cells with tumor reconstitution potential and cells with no tumor reconstitution potential. However, the tumor-reconstituting cells are not phenotypically the same as normal HSCs but are marked by an as yet undescribed cell marker (Figure 8, missing marker model). Alternatively, in many models, as assays have improved, it has become clear that leukemic cells with phenotypic features of transit amplifying cells have some level of self-renewal capacity. Thus, it is possible that AML cells do have limited differentiation that recapitulates normal myelopoiesis in some aspects, but the loss of stem cell potential that normally accompanies acquisition of lineage-specific markers is attenuated (Figure 8, modified differentiation model). Thus, as described in a murine model system, leukemic cells may simultaneously have features of differentiated progenitor cells and stem cells. The third alternative is that the stem cell model is fundamentally incorrect and that, in fact, all tumor cells retain the potential for tumor regeneration (Figure 8, tumor plasticity model). Proof of the first hypothesis would rest on discovery of an improved LSC marker and quantitative proof that selection for such a marker enhances for LSCs. Discrimination of the latter theory will require further quantitative analysis of engraftment potential in defined cell populations, which do or do not express differentiation markers. If the pattern is consistent that engraftment potential decreases with acquisition of lineage-specific markers, this would favor the hypothesis that leukemic maturation mirrors normal myelopoiesis but with a delayed loss of stem cell

CD38− cell populations. Thus, we have demonstrated that CD38+ cells meet the formal criteria for SL-ICs. Interestingly, in 5 out of 9 AML samples, the CD38+ fractions provided equal or superior engraftment levels compared with those obtained with CD38− fractions (using comparable injected cell numbers). This is particularly remarkable, considering that we, and others, have shown that anti-CD38 antibodies can decrease or even inhibit AML engraftment (21). Given this, our studies may underestimate the frequency of SL-ICs in CD38+ AML cell fractions.

In this report, we provide the first quantitative evaluation of the SL-ICs distribution as a function of cell surface phenotype. Our data and others indicate that SL-ICs may be most enriched in the Lin−CD34+/dimCD38− fraction. However, this fraction represents a small percentage of all AML cells in individual samples. We isolated 4 fractions based on Lin and CD38 expression and used limiting dilution analysis to determine the frequency and absolute numbers of SL-ICs found in each fraction. We found that, in one sample, 71% of all SL-ICs do not express CD38 and 29% of all AML-initiating cells reside in the CD38+ fraction. These results show that self-renewing SL-ICs with previously unrecognized phenotypes can represent a substantial portion of all SL-ICs in a patient. This has important implications for the development of curative therapies.

This study does not address the important question relating to the nature of the cell responsible for initiating AML. The phenotypic heterogeneity of SL-ICs and, in particular, our characterization

potential. On the other hand, if other AML samples actually demonstrate increased stem cell potential in populations expressing differentiation markers, this would suggest that leukemic cells do not recapitulate normal differentiation but are in a neomorphic state characterized by aberrant regulation of expression of differentiation markers. This type of plasticity is similar to that recently described for chemotherapy resistant cancer cells. Sharma et al. recently demonstrated that in cancer cell lines, chemotherapy resistance can track as a reversible trait secondary to epigenetic changes in cells over time (30). The discrimination between the 2 latter models may be dependent on the disease progression and treatment. At diagnosis, the stem cell model will fit with the modified differentiation model, while after chemotherapies, the stem cell theory will follow the tumor plasticity model. Further work should clarify these 2 latter models, but both models are in contrast to the original stem cell hypothesis, which completely restricted leukemic reconstitution potential to the immature cell fraction.

Methods

Primary cells. AML samples were obtained from the Stem Cell and Xenograft Core Facility at the University of Pennsylvania School of Medicine. Samples were obtained from patients presenting with acute myeloid leukemia at the Hospital of the University of Pennsylvania. Informed consent was obtained under a protocol reviewed and approved by the Institutional Review Board at the University of Pennsylvania. Leukopheresis samples were frozen in fetal calf serum with 10% DMSO and stored in liquid nitrogen. Samples that had previously shown high engraftment capability were chosen for this study (14). FAB or WHO classification and cytogenetics in AML samples were determined at time of diagnosis by the Laboratory of Pathology and Medicine at the Hospital of the University of Pennsylvania. Each collection was immunophenotyped using the following antibody panel: FITC-conjugated lineage cocktail 1 (CD3, CD14, CD16, CD19, CD20, and CD56), APC-conjugated anti-CD38, APC-Cy7-conjugated anti-CD45, PE-conjugated anti-CD44, PE–Texas Red–conjugated anti-CD33, PE-Cy5-conjugated anti-CD123, PE-Cy5.5-conjugated anti-CD34, and PE-Cy7-conjugated anti-CD45RA. All antibodies were purchased from BD Biosciences or Invitrogen. Analyses were performed on a BD Life Science Research II (LSR II) flow cytometer after cells were resuspended in a DAPI solution.

Mutational status. The mutational status of 8 genes (*FLT3*, *NPM1*, *WT1*, *CEBPA*, *KRAS*, *N-RAS*, *IDH1*, *IDH2*) was analyzed by high-resolution melting (HRM) methods (Table 1). DNA mutation screening of FLT3-TKD exon 20, IDH1 and IDH2 exon 4, N-RAS and KRAS exons 2 and 3, and WT1 exons 7 and 9 was performed by HRM PCR with the use of Light-Cycler 480 in High Melting Resolution Master Mix 1X (Roche Applied Science), with 10 ng genomic DNA, 0.1 μmol/l of each primer (see below), and 25 mmol/l MgCl2. HRM PCR cycling conditions were initial denaturation at 95°C for 10 minutes, followed by 50 cycles at 95°C for 10 seconds, 50 cycles at 63°C for 15 seconds, and 50 cycles at 72°C for 25 seconds. Melting curve was measured from 72°C to 95°C, with 25 acquisitions per degree centigrade. Primer sequences are as follows: FLT3_X20_F2, TCA-CAGAGACCTGGCCGC; FLT3_X20_R1, TGCCCCTGACAACATAGTT-GG; IDH1_X4_F1, GGCTTGTGAGTGGATGGGTAA; IDH1_X4_R2, GCATTTCTCAATTTCATACCTTGCTTA; IDH2_X4_F1, GAAAGAT-GGCGGCTGCAGT; IDH2_X4_R3, TGTTTTTGCAGATGATGGGC; NRAS_X2_F2, CTGATTACTGGTTTCCAACAGGTTCT; NRAS_X2_R2, TGGGTAAAGATGATCCGACAAGT; NRAS_X3_F1, TTGTTGGACATACT-GGATACAGCTG; NRAS_X3_R1, CATTTCCCCATAAAGATTCAGAA-CAC; KRAS_X2_F4, GGCCTGCTGAAAATGACTGAA; KRAS_X2_R4, AATTAGCTGTATCGTCAAGGCACTC; KRAS_X3_F2, TCCCTTCTCAG-GATTCCTACAGG; KRAS_X3_R2, ACAGGGATATTACCTACCTCATAAA-

CATT; WT1_X7_F2, CCCTCAAGACCTACGTGAATGTT; WT1_X7_R2, GGAGCTCTTGAACCATGTTTGC; WT1_X9_F1, TAGGGCCGAGGC-TAGACCTT; and WT1_X9_R1, TCTCATCACAATTTCATTCCACAATA. FLT3 exon 13 ITD and NPM1c mutation screening were performed using a multiplex PCR using Gold Taq DNA polymerase (Applied Biosystems) and the following primers: HsNPM1_X12_F1, 5′-GAAGTGTTGTGGTTCCT-TAAC; HsNPM1_X12_R1FAM, 5′(FAM) TGGACAACACATTCTTGGCA; FLT3_NEM_E, 5′ TGGTGTTTGTCTCCTCTTCATTGT 3′; and FLT3_NEM_Qned, 5′(NED) GTTGCGTTCATCACTTTTCCAA 3′. PCR products were analyzed on a sequencer using sizing fragment analysis. CEBPA screening was performed according to Pabst et al. (31).

Mice. Animals were used in accordance to a protocol reviewed and approved by the Institutional Animal Care and Use Committee of the University of Pennsylvania. NOD/LtSz-scid IL-2Rγchain[null] mice were produced at the University of Pennsylvania using breeders obtained from The Jackson Laboratory. Mice were housed and human primary AML cells were transplanted as reported previously (14). BM (mixed from tibias and femurs) and spleen were dissected in a sterile environment, flushed in PBS, and made into single cell suspensions for analysis by flow cytometry (FACS Calibur, BD) using FITC-conjugated anti-CD2, PE-conjugated anti-CD33, PerCP-Cy5.5-conjugated anti-CD19, and APC-conjugated anti-CD45 (all antibodies from BD) as well as using the LSR panel outlined above.

Limiting dilution analysis. Specific cell doses of 7 primary AML samples, ranging from 5×10^4 to 10×10^6 cells, were injected into at least 3 NSG mice per dose. Twelve to eighteen weeks after transplantation, the BM and the spleen were assessed for the engraftment. An engraftment criterion of more than 0.1% of human CD45+CD33+ in murine BM mononuclear cells assessed by flow cytometry was used as the biologically significant cutoff. The frequency of SL-ICs was calculated using Poisson statistics with the L-Calc Software for limiting dilution analysis (version 1.1; StemCell Technologies).

Cell sorting. Eight primary AML patient samples were stained with FITC-conjugated lineage cocktail 1 (CD3, CD14, CD16, CD19, CD20, and CD56), APC-conjugated anti-CD38, PE-conjugated anti-CD123, PE-Cy5.5-conjugated anti-CD34, and PE-Cy7-conjugated anti-CD45RA, before resuspension in a DAPI solution of PBS containing 2% FBS. Sorting was performed on a BD FACS Vantage SE/DiVa cell sorter, equipped with 3 lasers and 8 fluorescence detectors. High-speed cell sorting was performed within a BSL3 laboratory. Live gates were set up to exclude nonviable cells and debris with DAPI, and the forward scatter lineage-negative gate was defined as 5% of the live cell population expressing lineage markers at the lowest level. Purity checks were performed to ensure sort quality. The purities of the Lin−, Lin(dim), CD38−, CD38+, Lin−CD38−, Lin−CD38+, Lin(dim)CD38−, and Lin(dim)CD38+ fractions were 96.7% ± 2.1%, 96.2% ± 0.5%, 97.8% ± 1.9%, 95.9% ± 2.2%, 97.8% ± 1.2%, 95.9% ± 1.8%, 96.1% ± 2.0%, and 96.8% ± 1.5%, respectively (Supplemental Table 1). Highly purified subpopulations of 0.1 to 4 million cells were then injected into NSG mice. For 1 primary AML sample (sample 53), a LDA was performed on the 4 purified subpopulations of cells as well as the unprocessed cells. 1×10^4 to 5×10^6 cells were injected into 2–5 NSG mice. Nine to eighteen weeks after transplantation, the BM and the spleen were assessed for the engraftment. The frequency of SL-ICs was determined as described above.

Effect of anti-CD38 antibody on AML engraftment. Mononuclear cells from 1 AML patient sample (sample 53) were incubated overnight in fully supplemented endothelial growth medium (EGM-2; Lonza) at 37°C with anti-CD38 antibody (clone HIT2; BD) and isotype control (IgG1, clone MOPC-21; Sigma-Aldrich). After incubation, a 50-μl aliquot of each cohort was used to analyze the cell viability and the immunophenotypical frequency by LSR II flow cytometer using DAPI, FITC-conjugated lineage cocktail 1 (CD3, CD14, CD16, CD19, CD20, and CD56), APC-conjugated anti-CD38, APC-Cy7-conjugated anti-CD45, PE-conjugated anti-CD44, PE–Texas

Red–conjugated anti-CD33, PE-Cy5-conjugated anti-CD123, PE-Cy5.5-conjugated anti-CD34, and PE-Cy7-conjugated anti-CD45RA. The cell suspensions were centrifuged, resuspended in PBS containing 2% FBS, and injected into 5 irradiated NSG mice. Twelve weeks after transplantation, the BM and the spleen were assessed for engraftment by FACS analysis.

Secondary transplantation. Adult mice (8–10 weeks old) were sublethally irradiated with 250 cGy total body irradiation 24 hours prior to secondary transplantation. Engrafted BM samples were lysed with 0.8% ammonium chloride solution (StemCell Technologies), washed twice in PBS containing 2% FBS, and suspended in 200 μl PBS containing 2% FBS at a final concentration of 1 to 10 million human CD45+CD33+ viable cells from BM of primary recipients per mouse for intravenous injection. Twelve to eighteen weeks after transplantation, the BM and the spleen were assessed for the engraftment.

Hoechst 33342 and pyronin Y staining. Previously described methods were used with minor modifications (27, 32). Cryopreserved cells were thawed and 1 million of viable cells were incubated at 37°C (27) for 60 minutes in 1 ml Hanks buffered solution with 2% FBS and Hoechst 33342 at 5 μg/ml in presence of 100 μM verapamil. Pyronin Y was then added to a final concentration of 1 μg/ml, and incubation continued for another 30 minutes. Cells were washed in Hanks buffered solution with 2% FBS; then stained with 7AAD, FITC-conjugated lineage cocktail 1 (CD3, CD14, CD16, CD19, CD20, and CD56), APC-conjugated anti-CD34, APC-Cy5.5-conjugated anti-CD38, PE-Cy7-conjugated anti-CD45; and analyzed by LSR II flow cytometer (Becton Dickinson).

Statistics. We assessed the statistical analysis of the difference between 2 sets of data using nonparametric Mann-Whitney *U* test. *P* values of less than 0.05 were considered to be significant.

Address correspondence to: Martin Carroll, Division of Hematology/Oncology, Department of Medicine, University of Pennsylvania, BRB2/3, 421 Curie Blvd., Philadelphia, Pennsylvania 19104, USA. Phone: 215.573.5217; Fax: 215.573.7049; E-mail: carroll2@mail.med.upenn.edu.

1. Rosen JM, Jordan CT. The Increasing Complexity of the Cancer Stem Cell Paradigm. *Science.* 2009;324(5935):1670–1673.
2. Lapidot T, et al. A cell initiating human acute myeloid leukaemia after transplantation into SCID mice. *Nature.* 1994;367(6464):645–648.
3. Bonnet D, Dick JE. Human acute myeloid leukemia is organized as a hierarchy that originates from a primitive hematopoietic cell. *Nat Med.* 1997;3(7):730–737.
4. Al-Hajj M, Wicha MS, Benito-Hernandez A, Morrison SJ, Clarke MF. Prospective identification of tumorigenic breast cancer cells. *Proc Natl Acad Sci U S A.* 2003;100(7):3983–3988.
5. O'Brien CA, Pollett A, Gallinger S, Dick JE. A human colon cancer cell capable of initiating tumour growth in immunodeficient mice. *Nature.* 2007;445(7123):106–110.
6. Quintana E, Shackleton M, Sabel MS, Fullen DR, Johnson TM, Morrison SJ. Efficient tumour formation by single human melanoma cells. *Nature.* 2008;456(7222):593–598.
7. Ailles LE, Gerhard B, Kawagoe H, Hogge DE. Growth characteristics of acute myelogenous leukemia progenitors that initiate malignant hematopoiesis in nonobese diabetic/severe combined immunodeficient mice. *Blood.* 1999;94(5):1761–1772.
8. Lapidot T, Fajerman Y, Kollet O. Immune-deficient SCID and NOD/SCID mice models as functional assays for studying normal and malignant human hematopoiesis. *J Mol Med.* 1997;75(9):664–673.
9. Christianson SW, et al. Enhanced human CD4+ T cell engraftment in beta2-microglobulin-deficient NOD-scid mice. *J Immunol.* 1997;158(8):3578–3586.
10. Shultz LD, et al. Multiple defects in innate and adaptive immunologic function in NOD/LtSz-scid mice. *J Immunol.* 1995;154(1):180–191.
11. Feuring-Buske M, Gerhard B, Cashman J, Humphries RK, Eaves CJ, Hogge DE. Improved engraftment of human acute myeloid leukemia progenitor cells in beta 2-microglobulin-deficient NOD/SCID mice and in NOD/SCID mice transgenic for human growth factors. *Leukemia.* 2003;17(4):760–763.
12. Shultz LD, et al. Human lymphoid and myeloid cell development in NOD/LtSz-scid IL2R gamma null mice engrafted with mobilized human hemopoietic stem cells. *J Immunol.* 2005;174(10):6477–6489.
13. Ishikawa F, et al. Development of functional human blood and immune systems in NOD/SCID/IL2 receptor {gamma} chain(null) mice. *Blood.* 2005;106(5):1565–1573.
14. Sanchez PV, et al. A robust xenotransplantation model for acute myeloid leukemia. *Leukemia.* 2009;23(11):2109–2117.
15. Ishikawa F, et al. Chemotherapy-resistant human AML stem cells home to and engraft within the bone-marrow endosteal region. *Nat Biotechnol.* 2007;25(11):1315–1321.
16. Berenson RJ, et al. Antigen CD34+ marrow cells engraft lethally irradiated baboons. *J Clin Invest.* 1988;81(3):951–955.
17. Terstappen LW, Huang S, Safford M, Lansdorp PM, Loken MR. Sequential generations of hematopoietic colonies derived from single nonlineage-committed CD34+CD38- progenitor cells. *Blood.* 1991;77(6):1218–1227.
18. Bhatia M, Wang JC, Kapp U, Bonnet D, Dick JE. Purification of primitive human hematopoietic cells capable of repopulating immune-deficient mice. *Proc Natl Acad Sci U S A.* 1997;94(10):5320–5325.
19. Lapidot T, et al. A cell initiating human acute myeloid leukaemia after transplantation into SCID mice. *Nature.* 1994;367(6464):645–648.
20. Bagg A. Lineage ambiguity, infidelity, and promiscuity in immunophenotypically complex acute leukemias: genetic and morphologic correlates. *Am J Clin Pathol.* 2007;128(4):545–548.
21. Taussig DC, et al. Anti-CD38 antibody-mediated clearance of human repopulating cells masks the heterogeneity of leukemia-initiating cells. *Blood.* 2008;112(3):568–575.
22. Jin L, et al. Monoclonal antibody-mediated targeting of CD123, IL-3 receptor alpha chain, eliminates human acute myeloid leukemic stem cells. *Cell Stem Cell.* 2009;5(1):31–42.
23. Jin L, Hope KJ, Zhai Q, Smadja-Joffe F, Dick JE. Targeting of CD44 eradicates human acute myeloid leukemic stem cells. *Nat Med.* 2006;12(10):1167–1174.
24. Hosen N, et al. CD96 is a leukemic stem cell-specific marker in human acute myeloid leukemia. *Proc Natl Acad Sci U S A.* 2007;104(26):11008–11013.
25. Taussig DC, et al. Leukemia-initiating cells from some acute myeloid leukemia patients with mutated nucleophosmin reside in the CD34(-) fraction. *Blood.* 2010;115(10):1976–1984.
26. Manz MG, Miyamoto T, Akashi K, Weissman IL. Prospective isolation of human clonogenic common myeloid progenitors. *Proc Natl Acad Sci U S A.* 2002;99(18):11872–11877.
27. McKenzie JL, Gan OI, Doedens M, Dick JE. Reversible cell surface expression of CD38 on CD34-positive human hematopoietic repopulating cells. *Exp Hematol.* 2007;35(9):1429–1436.
28. Blair A, Hogge DE, Sutherland HJ. Most acute myeloid leukemia progenitor cells with long-term proliferative ability in vitro and in vivo have the phenotype CD34(+)/CD71(-)/HLA-DR. *Blood.* 1998;92(11):4325–4335.
29. Barabe F, Kennedy JA, Hope KJ, Dick JE. Modeling the initiation and progression of human acute leukemia in mice. *Science.* 2007;316(5824):600–604.
30. Sharma SV, et al. A chromatin-mediated reversible drug-tolerant state in cancer cell subpopulations. *Cell.* 2010;141(1):69–80.
31. Pabst T, et al. Dominant-negative mutations of CEBPA, encoding CCAAT/enhancer binding protein-alpha (C/EBPalpha), in acute myeloid leukemia. *Nat Genet.* 2001;27(3):263–270.
32. Guan Y, Gerhard B, Hogge DE. Detection, isolation, and stimulation of quiescent primitive leukemic progenitor cells from patients with acute myeloid leukemia (AML). *Blood.* 2003;101(8):3142–3149.